Analytical Expressions of Hydro-Seismic Forces on Dams

Abdelmadjid Tadjadit[1], Boualem Tiliouine[1*]

Abstract

Analytical expressions for the determination of hydro-seismic forces acting on a rigid dam with irregular upstream face geometry in presence of a compressible viscous fluid are derived through a linear combination of the natural modes of water in the reservoir based on a boundary method making use of complete sets of complex T-functions.

The formulas obtained for distributions of both shear forces and overturning moments are simple, computationally effective and useful for the preliminary design of dams. They show clearly the separate and combined effects of compressibility and viscosity of water. They also have the advantage of being able to cover a wide range of excitation frequencies even beyond the cut-off frequencies of the natural modes of the reservoir. Key results obtained using the proposed analytical expressions of the hydrodynamic forces are validated using numerical and experimental solutions published for some particular cases available in the specialized literature.

1 Civil Engineering Department, Ecole Nationale Polytechnique,
  10 Avenue H. Badi, 16200, Algiers, Algeria
* Corresponding author, email: boualem.tiliouine@g.enp.edu.dz

1 Introduction

Dams were historically built to meet the vital needs such as drinking water supply, irrigation and electrical power generation. They are, therefore, very sensitive works requiring high protection against hydrodynamic forces which are important factors in seismic design considerations during earthquakes. Failure of dams can cause uncontrollable damage, not only to properties, but also to populations.

The analysis and design of this particular class of structures may prove to be a difficult task as it involves the combination of knowledge of several disciplines such as fluid mechanics, solid mechanics, hydrodynamics, wave propagation...etc. Analytical expressions of hydrodynamic forces on dams are rare and available only under simple geometry of the water dam interface. Several works: analytical, experimental and numerical, have been devoted in order to obtain an accurate determination of the hydrodynamic pressures exerted on dams during earthquakes. Westergaard [1] was the pioneer to have derived an analytical expression to evaluate the hydrodynamic pressures applied to a rigid dam with vertical upstream face under a horizontal harmonic ground motion. Using the electric analog method, Zangar [2] studied experimentally the hydrodynamic effect of horizontal earthquake action on a rigid dam having upstream face with either constant or compound slopes in the presence of an incompressible fluid. Chopra [3] published an analytical solution for vertical rigid dams under horizontal and vertical earthquake ground motions taking into account the effect of compressibility of the fluid in the reservoir. Chwang [4], based on "Two-Dimensional potential-flow theory" obtained the exact solution for earthquake forces on a rigid dam with an inclined upstream face of constant slope in presence of an incompressible inviscid fluid. Liu [5], using the same theory obtained analytical solution for the hydrodynamic pressures acting on the inclined upstream dam face for different bottom slopes. Tsai [6] developed a semi analytical solution for hydrodynamic pressure distribution on rigid dams with arbitrary upstream face considering water compressibility. Moreover several authors have used the numerical methods essentially based on the F.E.M, to include the effects of compressibility of the fluid in the reservoir

[7, 8, 9], the flexibility of the dam [10, 11] and pressure wave absorption by sediments at the bottom of the reservoir [12, 13, 14]. Additively to these numerical methods, there are also, semi-analytical ones. They remain valid and are an important input for the preliminary dam design [6, 15, 16].

In this paper, analytical expressions for the determination of hydro-seismic forces acting on a rigid dam with irregular upstream face geometry in presence of a compressible viscous fluid are derived through a linear combination of the natural modes of water in the reservoir based on a boundary method making use of complete sets of complex T-functions. Key results obtained using the proposed analytical expressions of the hydrodynamic forces are validated using numerical and experimental solutions published for some particular cases available in the specialized literature.

2 Background
2.1 Assumptions

Consider a rigid dam with partially inclined upstream face impounded by a reservoir of infinite length and rigid bottom subjected to horizontal earthquake short durations. Coordinate origin is located at the base of the dam (Fig. 1). The motion of the dam-reservoir system is two-dimensional and the water in the reservoir is considered linearly compressible, viscous and irrotational.

Let M (x, y) be a point in the Cartesian coordinate system (o, x, y), located at the upstream face of the dam at an elevation y from the reservoir bottom; the coordinates of the point M are:

$$x = \begin{cases} (CH - y)\tan\theta & y < CH \\ 0 & y \geq CH. \end{cases} \quad (1)$$

where, H is the depth of the water in the reservoir; C is the fraction of height H and θ the angle formed by the inclined portion of the upstream face with the vertical.

Since the dam undergoes a displacement of rigid body, consequently the set of points belonging to the fluid-structure interface are assumed to have, at each time, the same acceleration as the base of the dam.
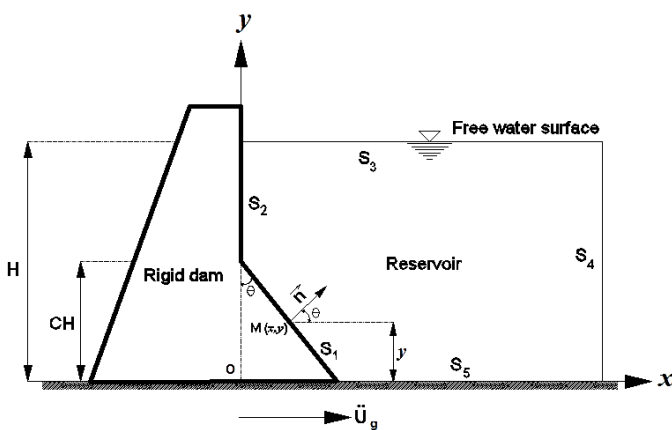
Fig. 1 Rigid dam with partially inclined face and infinite length reservoir subjected to a horizontal ground motion

On Fig. 1, the reservoir is delimited by four contours defined as:

$S_1 \cup S_2$: Contour delimiting the upstream face of the dam; S_3: Contour defining the free surface of water; S_4: Contour defining the boundary of truncation of the reservoir and S_5: Contour defining the reservoir bottom.

CH is defined as the height of the inclined portion of the upstream face and $\vec{n}$ is the outward normal direction to the dam-water interface.

2.2 Formulation of governing equation

The hydrodynamic pressure in excess of the hydrostatic pressure in the reservoir is governed by the equation of the compression waves given as follows:

$$\nabla^2 p = \left(\frac{1}{c^2}\right)(\partial^2 p / \partial t^2). \quad (2)$$

where:

$$\nabla^2 = \partial^2 / \partial x^2 + \partial^2 / \partial y^2. \quad (3)$$

corresponds to the two dimensional Laplace operator in Cartesian coordinates with:

$$c = \sqrt{\lambda / \rho}. \quad (4)$$

In equation (4), c represent the speed of sound waves in water, λ the Lamé's modulus and ρ the mass density of water.

Since we are assuming small deformations and considering the combined effects of compressibility and viscosity of the fluid in the reservoir, the linear visco-elastic Kelvin-Voigt model [17] was adopted to represent the internal dissipation. Lamé's modulus is then expressed by a complex valued function depending on the angular frequency of excitation w and it is given by Eq. (5). Well understood, this way of doing would make it possible to simulate the internal damping which causes a loss of energy for the compression waves traveling away from the dam.

$$\lambda^c = \lambda(1 + i2\eta\xi). \quad (5)$$

where $\eta = wH/c$ is the dimensionless frequency; w is the angular frequency of the excitation and ξ the fraction of the critical damping of water.

It is assumed that the dam vibrates as a rigid body with the same horizontal ground acceleration given as follows:

$$\ddot{U}_g(t) = e^{iwt}. \quad (6)$$

since we have contemplated a simplified seismic evaluation approach, the peak ground acceleration is considered sufficient to define the seismic parameters [18].

As previously advanced, the pressure in the reservoir can be given in the frequency domain as:

$$p = P(x, y, w)e^{iwt}. \quad (7)$$

Substituting Eq. (7) in Eq. (2) provides:

$$\partial^2 P / \partial x^2 + \partial^2 P / \partial y^2 + K^2 P = 0. \tag{8}$$

Equation (8) represents the Helmholtz differential equation of compression waves in the water and $K = w/c$, corresponds to the compression wave number.

2.3 Boundary conditions

The boundaries conditions for the dam-reservoir system shown in Fig. 1 are given by:

1. On the upstream part of the dam enclosed by the contour $S_1 \cup S_2$, it is assumed that the hydrodynamic pressures gradient in the direction normal to the upstream face of the dam and the inertial forces generated in the mass of the water are in a state of equilibrium, which allows us to write:

$$\partial P(x,y,w) / \partial n|_{S_1 \cup S_2} = -\rho \ddot{U}_n. \tag{9}$$

where $\ddot{U}_n$ is the normal component of the horizontal ground acceleration given as:

$$\ddot{U}_g = \begin{cases} \ddot{U}_g \cos\theta & y < CH \\ \ddot{U}_g & y \geq CH. \end{cases} \tag{10}$$

2. At the free surface of water, we assume that $P(x,H,W)|_{S_3} = 0$.

3. At the limit of truncation S_4, supposed far enough from the dam upstream face (when $L \geq 3H$; L is the length of the reservoir), we assume that $P(\infty, y, w)|_{S_4} = 0$ [10].

4. At the reservoir bottom, acceleration of particles of the water in the vertical direction is null and the gradient of associated hydrodynamic pressures is also zero:

$$\partial P(x,0,w) / \partial y|_{S_5} = 0. \tag{11}$$

3 Analytical expression for distribution of the total shear forces

Under a horizontal seismic loading, the hydrodynamic pressure $P(x, y, w)$ is given by the following relationship:

$$P = \sum_{i=1}^{+\infty} A_i T_i(x,y,w) = C_s \gamma H C_p. \tag{12a}$$

with

$$T_i(x,y,w) = e^{-\mu_i x} \cos\lambda_i y. \tag{12b}$$

where, $T_i(x, y, w)$ define the natural water modes of vibration in the reservoir propagating horizontally, $C_s = \ddot{U}_n/g$, g is the acceleration of gravity, γ is the unit weight of water and C_p the pressure coefficient. Here, C_p is approximated by a series of complex functions of real variable y belonging on the compact interval $I = [0, H]$ as follows:

$$C_p(y)|_{S_1 \cup S_2} = (1/C_s \gamma H) \sum_{i=1}^{+\infty} A_i e^{-\mu_i x} \cos\lambda_i y. \tag{13}$$

where, $\lambda_i = (2i-1)\pi/2H$ and $\mu_i = \sqrt{\lambda_i^2 - K^2}$.

A_i, correspond to the unknown coefficients with i = 1, 2, …, ∞. They are obtained after solving a system of linear equations given by the relation below (Eq. (14)) using a numerical calculation program developed for this purpose.

$$[F_{ji}]\{A_i\} = \{G_j\} \quad \forall \ j, i = 1, 2, \ldots \infty. \tag{14}$$

The elements of the Hermitian matrix $[F_{ji}]$ and the column vector $\{G_j\}$ are calculated as defined in [15]. For a computational tolerance of 10^{-4}, beyond 25 terms, the uniform convergence of the series of functions $C_p(y)$ is verified through the "Uniform Cauchy criterion". The latter converges to a called "Limit function" defined as the set of points corresponding to the simple convergence sequences at any point y of the compact interval [0, H].

Thus, under the above conditions, an approximate solution will be obtained for Eq. (13) for a finite number of terms.

The distribution of the horizontal component of the total shear forces along the contour $S_1 \cup S_2$ is given as follow:

$$F_h(y) = \int_S C_s \gamma H C_p ds. \tag{15}$$

where, ds represent infinitely small segment of the $S_1 \cup S_2$ boundary.

Substituting Eq. (13) into Eq. (15), yields:

$$F_h(y) = \int_y^H \sum_{i=1}^{+\infty} A_i e^{-\mu_i x} \cos\lambda_i y \ dy. \tag{15a}$$

Since the pressure response is given as a series of continuous functions converging uniformly on [0, H], an interchange between the operator ($\int$) and the operator ($\sum$) is permitted.

Thus, Eq. (15 a) takes the following form:

$$F_h(y) = \sum_{i=1}^{+\infty} A_i \int_y^H e^{-\mu_i x} \cos\lambda_i y \ dy. \tag{15b}$$

After successive integrations, we finally obtain:
for $y \in [0, CH]$

$$F_h(y) = \sum_{i=1}^{+\infty} A_i \left\{ \begin{array}{c} -e^{-\gamma_i(CH-y)} F_i(y) \\ + F_i(CH) \\ + \dfrac{[\sin\lambda_i H - \sin\lambda_i CH]}{\lambda_i} \end{array} \right\}. \tag{16a}$$

for $y \in [CH, H]$

$$F_h(y) = \sum_{i=1}^{+\infty} A_i \{[\sin\lambda_i H - \sin\lambda_i y]/\lambda_i\}. \tag{16b}$$

with:

$$F_i(y) = (\lambda_i \sin\lambda_i y + \mu_i \tan\theta \cos\lambda_i y)/\alpha_i^+,$$
$$F_i(CH) = (\lambda_i \sin\lambda_i CH + \mu_i \tan\theta \cos\lambda_i CH)/\alpha_i^+,$$
$$\gamma_i = \mu_i \tan\theta, \quad \alpha_i^+ = \lambda_i^2 + \gamma_i^2 \ and \ \alpha_i^- = \lambda_i^2 - \gamma_i^2.$$

In Eq. (16 a) and Eq. (16 b), $F_h(y)$ represents the horizontal component of the total shear force above any elevation y of the bottom of the reservoir.

4 Analytical expression for distribution of the overturning moments

The distribution of the total overturning moments about the Z axis at any elevation y generated by the horizontal shear forces is defined as:

$$M_z(y) = \int_S F_h(y)\,ds. \tag{17}$$

After successive integrations, Eq. (17) becomes:

for $y \in [0, CH]$

$$M_Z(y) = \sum_{i=1}^{+\infty} A_i \left\{ \begin{array}{l} e^{-\gamma_i(CH-y)} M_i(y) - M_i(CH) + \\ (CH-y)\left[\begin{array}{l} (\lambda_i \sin \lambda_i CH + \gamma_i \cos \lambda_i CH)/\alpha_i^+ \\ +(\sin \lambda_i H - \sin \lambda_i CH)/\lambda_i \end{array} \right] \\ + \dfrac{\left[\lambda_i H(1-C)\sin \lambda_i H - \cos \lambda_i CH\right]}{\lambda_i^2} \end{array} \right\}. \tag{18a}$$

for $y \in [CH, H]$

$$M_z(y) = \sum_{i=1}^{+\infty} A_i \left\{ \left[\lambda_i(H-y)\sin \lambda_i H - \cos \lambda_i y\right]/\lambda_i^2 \right\}. \tag{18b}$$

with:

$$M_i(y) = \left[m_i \sin \lambda_i y + n_i \cos \lambda_i y\right]/\alpha_i^{+2},$$
$$M_i(CH) = \left[m_i \sin \lambda_i CH + n_i \cos \lambda_i CH\right]/\alpha_i^{+2}$$
$$m_i = 2\lambda_i \gamma_i \text{ and } n_i = -\alpha_i^-.$$

In Appendix A, simplified formulas are given for some specific geometric configurations of the dam-water interface. The maximum values of $F_h(y)$ and $M_z(y)$ are also computed at the bottom of the reservoir. For illustration purposes, graphical representations of the mode shapes of the 1st, 2nd and the 3rd natural water modes of vibration in the reservoir are also presented. In Appendix B, we have presented for a specific case study, the values of the Hermitian matrix $[F_{ji}]$, the column vector $\{G_j\}$ and the column vector of the unknown coefficients $\{A_i\}$.

5 Results and discussion

In order to implement the proposed analytical formulas, a computer program in Matlab language [16] was modified to incorporate, in the frequency-domain, the effects of compressibility and viscosity of water in the reservoir. Initially, the program considered only the case of an incompressible inviscid fluid.

Results obtained for total shear forces and overturning moments are expressed, respectively, in terms of dimensionless coefficients $CF = |F_h|/F_{st}$ and $CM = |M_z|/M_{st}$ in which $|F_h|$ and $|M_z|$ are the modulus of the complex frequency responses of F_h and M_z. $F_{st} = \rho g H^2/2$ and $M_{st} = \rho g H^3/6$ are respectively, the total hydrostatic force and the corresponding overturning moment at the base of the dam. Pressures, shear forces and associated overturning moments are, respectively expressed, in Pascal, Newton and Newton-meter per unit of width of the dam.

Several results are obtained corresponding to different geometries of dam-water interfaces and different values of the damping ratio ξ over a wide range of excitation frequencies w.

The first numerical application was for a rigid dam with vertical upstream face (C = 0 or $\theta = 0$), impounded by a reservoir with compressible undamped water. In order to compare the numerical results obtained with those given by Westergaard, we consider the case of a harmonic ground excitation with period T = 4/3 sec and a sound wave speed in water $c = 1438$ m/s. As one can observe from Table 1, the numerical results obtained are in a very good agreement with those given by the exact method of Westergaard.

Table 1 Percent errors of p, F_h and M_z between analytical expressions and the exact method of Westergaard

	Reservoir depth H(m)		
	60.96	182.88	243.84
$p(\%)$	0,024	0,032	0,014
$F_h(\%)$	−0,044	0,037	−0,056
$M_z(\%)$	−0,027	−0,005	−0,040

However, the same comparison was made with the assumption of an incompressible fluid [16], the relative errors recorded were more important, especially for reservoirs of large heights, where the effect of compressibility is more pronounced. In fact, as the height of the water level increases, the fundamental frequency of the reservoir given by $w_1 = \pi c/2H$ decreases and approaches more and more the excitation frequency ($w = 2\pi/T$). On the other hand, for reservoirs of low height, it would be necessary to have a high excitation frequency level in order to be able to highlight the effect of the compressibility of the fluid in the reservoir.

To further illustrate this situation, two other comparisons were made; the first with respect to the experimental method of Zangar [2] and the second with respect to that of the exact method of Chwang [4]. For these two authors, the fluid is considered incompressible; the results obtained are summarized in Tables 2 and 3, which clearly show that the percent errors increase progressively with the increase of the water height level in the reservoir.

Table 2 Percent errors of p, F_h and M_z between analytical expressions and experimental method of Zangar

	Reservoir depth H(m)		
	60.96	182.88	243.84
$p(\%)$	1.903	9.968	18.711
$F_h(\%)$	2.502	9,700	17.343
$M_z(\%)$	−0.174	6.237	13.031

Table 3 Percent errors of p, F_h between analytical expressions and the exact method of Chwang

	Reservoir depth H(m)		
	60.96	182.88	243.84
$p(\%)$	0.874	8.857	17.512
$F_h(\%)$	0.729	7.803	15.314
$M_z(\%)$	-	-	-

In the following applications, the results obtained were presented for a wide range of values of the dimensionless frequency η and different damping ratios ξ of the water. The Characteristic parameters of the dam-reservoir system are: $\rho = 1000 \ kg/m^3$ and $C_s = 0.1$ (Signal of unit amplitude equal to $1 \ m/s^2$ with variable frequency covering the range of values of the seismic frequencies).

In figures 2 and 3, both real and imaginary parts of CF are presented for the dimensionless frequencies $\eta = 0$, 1.5, 3 and 6. We can easily see the effect of the excitation frequency on the response of the system. When η exceeds $\pi/2$, the response is complex valued with the imaginary part representing the loss of energy in waves moving away from the dam.
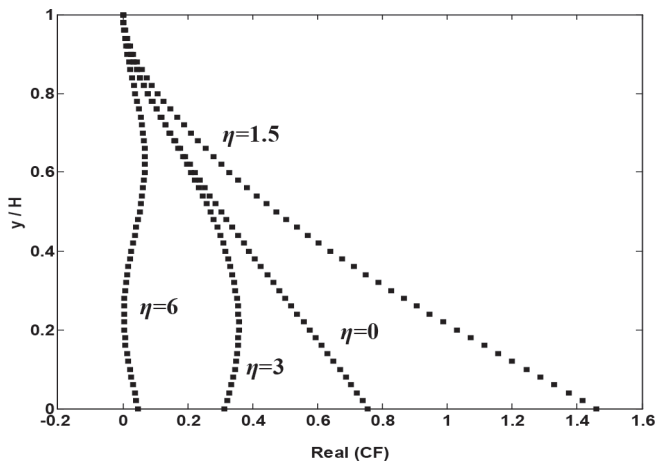
Fig. 2 Real parts of total shear forces on a rigid dam with sloping angle $\theta = 37.6°$ and C = 0.75 (undamped fluid case, $\xi = 0\%$)
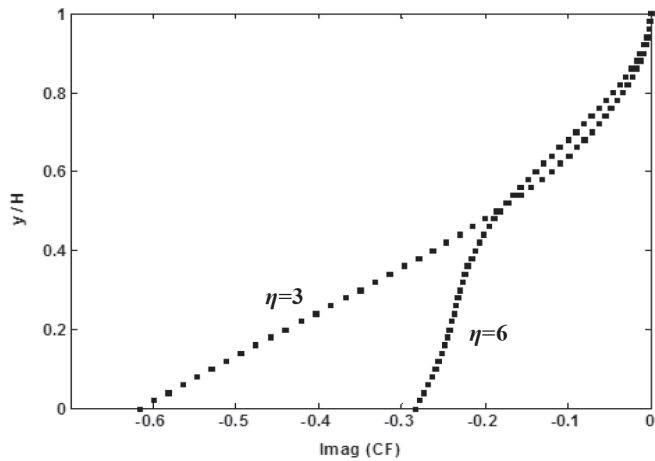
Fig. 3 Imaginary parts of total shear forces on a rigid dam with sloping angle $\theta = 37.6°$ and C = 0.75 (undamped fluid case, $\xi = 0\%$)

The same reasoning can be adopted for the distribution of the total overturning moments (Fig. 4 and 5).

It can be noted that, contrarily to hydrodynamic pressures, whatever the configuration of the upstream face, the maximum values of the hydrodynamic forces always occur at the base of the dam.
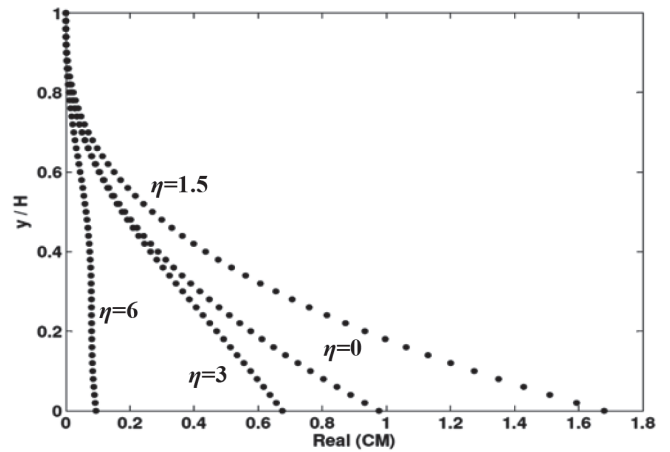
Fig. 4 Real parts of total overturning moments on a rigid dam with sloping angle $\theta = 37.6°$ and C = 0.75 (undamped fluid case, $\xi = 0\%$)
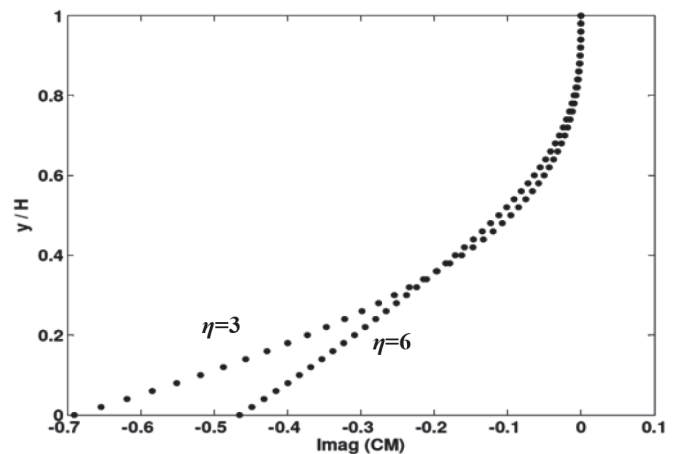
Fig. 5 Imaginary parts of total overturning moments on a rigid dam with sloping angle $\theta = 37.6°$ and C = 0.75 (undamped fluid case, $\xi = 0\%$)

Now, to evaluate the combined effects of compressibility and viscosity of water, another example is given for the case of a vertical rigid dam.
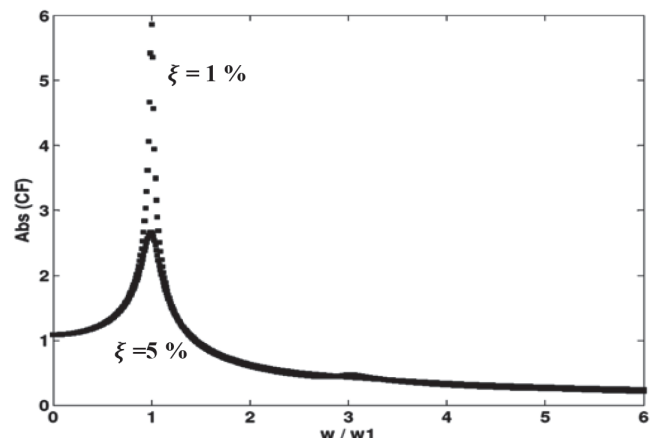
Fig. 6 Total shear forces on a rigid dam with a vertical upstream face for damping ratios $\xi = 1\%$ and $\xi = 5\%$

Figure 6 shows the variation of the dimensionless coefficient CF with the frequency ratio w/w_1 for damping ratios $\xi = 1\%$ and $\xi = 5\%$. It is seen that the effect of water viscosity can be considered negligible insofar as the excitation frequency is not very close to that of the fundamental modes of the reservoir.

In the following, the study is extended to the case of an inclined dam formed by two plane upstream faces with a sloping angle $\theta = 37.6°$ and height ratio C = 0.75, taking into account the effects of both compressibility and viscosity of water. In figure 7, we can note the consistency of the trends between the results obtained and those given by Avilés [15].
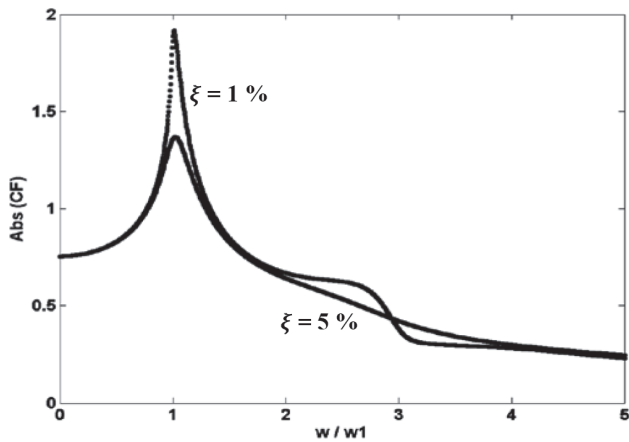
Fig. 7 Total shear forces on a partially inclined dam with sloping angle θ = 37.6° and C = 0.75, for damping ratios ξ = 1% and ξ = 5%
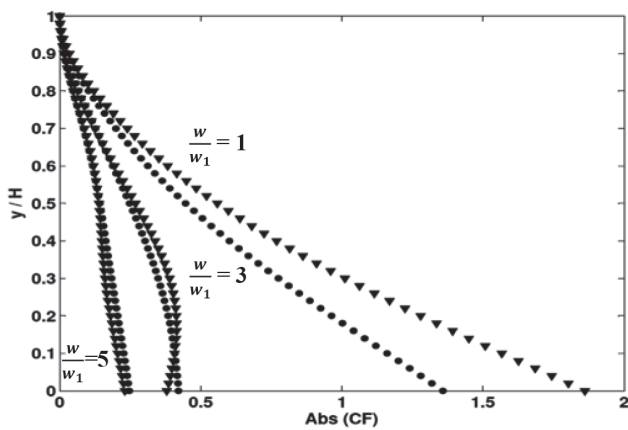
Fig. 8 Distribution of total shear force on a partially inclined dam with sloping angle θ = 37.6° and C = 0.75, for damping ratios ξ = 1% (Triangle marker) and ξ = 5% (Circle marker)
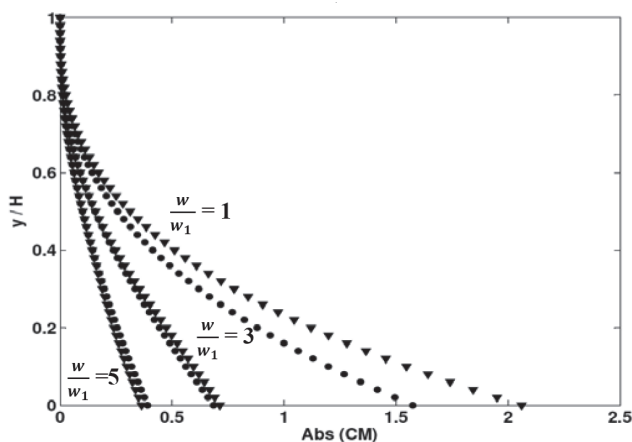
Fig. 9 Distribution of total overturning moments on a partially inclined dam with sloping angle θ = 37.6° and C = 0.75, for damping ratios ξ = 1% (Triangle marker) and ξ = 5% (Circle marker)

In figures 8 and 9, the distributions of normalized hydro-seismic forces and overturning moments are presented for dimensionless frequencies $w/w_1 = 1, 3$ and 5. As one can observe, largest effects of viscosity of water occur for the fundamental mode of vibration of the reservoir. We also can observe that the lower the excitation frequency, the greater the influence of the effect of water viscosity.

6 Conclusions

Analytical expressions for the determination of hydro-seismic forces acting on a rigid dam with irregular upstream face geometry in presence of a compressible viscous fluid are derived through a linear combination of the natural modes of water in the reservoir based on a boundary method making use of complete sets of complex T-functions. They show clearly the separate and combined effects of compressibility and viscosity of water.

The numerical results obtained are very consistent with those given by Westergaard when the dam upstream face is vertical. The effect of water compressibility is shown by comparing the results with those obtained by Zangar and Chwang respectively. The study was then extended to the case of a rigid dam with irregular geometry in presence of compressibility and viscosity of the water. The results obtained were presented for a wide range of values of the dimensionless frequency η and different damping ratios ξ of the water.

In the case of high rigid dams and high values of excitation frequencies, the importance of effect of compressibility on the total hydrodynamic pressures, shear forces and associated overturning moments is not identical. When compressibility effect is neglected, the percent errors, in the present study, are found to be in the order of 15–18 % for hydrodynamic pressures, 14–17 % for shear forces and less than 13 % for overturning moments.

In general, the effect of viscosity of the water may be neglected insofar as the frequency of the seismic excitation is not very close to that of the natural modes of vibration of the reservoir. However, at the resonance frequency, the generalized seismic forces are controlled essentially by the damping ratio of the water in the reservoir.

The formulas obtained for distributions of both shear forces and overturning moments are simple, computationally effective and useful for the preliminary design of dams. They also have the advantage of being able to cover a wide range of excitation frequencies even beyond the cut-off frequencies of the natural water modes of the reservoir.

References

[1] Westergaard, H. M. "Water pressures on dams during earthquakes". *Transactions of the American Society of Civil Engineers*, 98(2), pp. 418–472. 1933.

[2] Zangar, C. N. "Hydrodynamic pressures on dams due to horizontal earthquakes". *Proceedings of the Society for Experimental Stress Analysis*, 10, pp. 93–102. 1953.

[3] Chopra, A. K. "Hydrodynamic pressures on dams during earthquakes". *Journal of the Engineering Mechanics Division*, 93(6), pp. 205–223. 1967.

[4] Chwang, A. T. "Hydrodynamic pressures on sloping dams during earthquakes. Part 2. Exact theory". *Journal of Fluid Mechanics*, 87(2), pp. 343–348. 1978. https://doi.org/10.1017/S0022112078001640

[5] Liu P. L. F. "Hydrodynamic pressures on rigid dams during earthquakes". *Journal of fluid mechanics*, 165, pp. 131–145. 1986. https://doi.org/10.1017/S0022112086003026

[6] Tsai, C. S. "Semi-analytical solution for hydrodynamic pressures on dams with arbitrary upstream face considering water compressibility". *Computers and Structures*, 42(4), pp. 497–502. 1992. https://doi.org/10.1016/0045-7949(92)90117-I

[7] Hall, J. F., Chopra, A. K. "Hydrodynamic effects in earthquake response of embankment dams". *Journal of Geotechnical Engineering Division*, 108(4), pp. 591–597. 1982.

[8] Sharan, S. K. "A non-reflecting boundary in fluid-structure interaction". *Computers and Structures*, 26(5), pp. 841–846. 1987. https://doi.org/10.1016/0045-7949(87)90034-4

[9] Tiliouine, B., Seghir, A. "A numerical model for time domain analysis of dams including fluid-structure interaction". In : *CST 98 International Conference*, Edinburgh. Scotland, Aug. 18–20, 1998. http://www.freewebs.com/seghir/Pubs/CST98.pdf

[10] Tiliouine, B., Seghir, A. "Fluid-structure models for dynamic studies of dam-water systems". In : *Eleventh European Conference on Earthquake Engineering*, Paris, France, Sep. 6–11. 1998. http://www.freewebs.com/seghir/Pubs/ECEE98.pdf

[11] Gogoi, I., Maity, D. "A novel procedure for determination of hydrodynamic pressure along upstream face of dams due to earthquakes". *Computers and Structures*, 88(9–10), pp. 539–548. 2010. https://doi.org/10.1016/j.compstruc.2010.01.007

[12] Fenves, G., Chopra, A. K. "Effects of reservoir bottom absorption and dam-water-foundation rock interaction of the frequency response functions for concrete gravity dams". *Journal of Earthquake Engineering and Structural Dynamics*, 13(1), pp. 13–31. 1985. https://doi.org/10.1002/eqe.4290130104

[13] Kianoosh, H. "Effect of reservoir bottom on earthquake response of concrete dams". *Soil Dynamics and Earthquake Engineering*, 16(7), pp. 407–415. 1997. https://doi.org/10.1016/S0267-7261(97)00023-7

[14] Li Shang-Ming, Liang Hong, Li Ai-min. "A semi-analytical solution for characteristics of a dam-reservoir system with absorptive reservoir bottom". *Journal of Hydrodynamics*, 20(6), pp. 727–734. 2008. https://doi.org/10.1016/S1001-6058(09)60008-1

[15] [15] Avilés, J., Li, X. "Analytical–numerical solution for hydrodynamic pressures on dams with sloping face considering compressibility and viscosity of water". *Computers and Structures*, 66(4), pp. 481–488. 1998. https://doi.org/10.1016/S0045-7949(97)00091-6

[16] Tadjadit, A., Tiliouine, B. "Analytical formulation of hydro-seismic forces at the fluid-structure interface of rigid dams with irregular upstream face under seismic excitations" (in French). *Romanian Journal of Technical Sciences, Applied Mechanics*, 58(3), pp. 287–298. 2013.

[17] Newmark, N. M., Rosenblueth, E. "*Fundamentals of Earthquake Engineering*". Prentice–Hall, Englewood Cliffs, NJ, pp. 177-212. 1971.

[18] International commission on large dams. "Selecting seismic parameters for large dams". Bulletin 148. (Revision of Bulletin 72). 2016.

Appendix A

1. Special cases for the distributions of $F_h(y)$ and $M_z(y)$
1.1 Rigid dam with sloping upstream face

$$F_h(y) = \sum_{i=1}^{+\infty} A_i \left[-e^{-\gamma_i(H-y)} F_i(y) + F_i(H) \right]. \tag{A1}$$

with

$$F_i(y) = \frac{\left[\lambda_i \sin \lambda_i y + \mu_i \tan\theta \, \cos\lambda_i y \right]}{\alpha_i^+},$$

$$F_i(H) = \left[\lambda_i \sin \lambda_i H + \mu_i \tan\theta \, \cos\lambda_i H \right] / \alpha_i^+,$$

$$M_Z(y) = \sum_{i=1}^{+\infty} A_i \begin{bmatrix} e^{-\gamma_i(H-y)} M_i(y) - M_i(H) \\ + \left[\lambda_i (H-y) \sin \lambda_i H \right] / \alpha_i^+ \end{bmatrix}. \tag{A2}$$

with

$$M_i(y) = \frac{\left[m_i \sin \lambda_i y + n_i \cos\lambda_i y \right]}{\alpha_i^{+2}},$$
$$M_i(H) = m_i \sin \lambda_i H / \alpha_i^{+2}.$$

1.2 Rigid dam with vertical upstream face

In this case we have:

$$\alpha_i^+ = \alpha_i^- = \lambda_i^2 \ and \ \gamma_i = 0,$$

$$F_h(y) = \sum_{i=1}^{+\infty} \frac{A_i}{\lambda_i} \left[\sin \lambda_i H - \sin \lambda_i y \right], \tag{A3}$$

$$M_Z(y) = \sum_{i=1}^{+\infty} \frac{A_i}{\lambda_i^2} \left[-\cos \lambda_i y + \lambda_i (H - y) \sin \lambda_i H \right]. \tag{A4}$$

2. Maximum values of the total shear forces and overturning moments

The maximum values of the total shear forces and the associated overturning moments are given at the base of the dam ($y = 0$) as follows:

$$F_h(0) = \sum_{i=1}^{+\infty} A_i \left\{ \begin{array}{l} -\mu_i \tan\theta \ e^{-\gamma_i CH} / \alpha_i^+ + F_i(CH) + \\ \left[\sin \lambda_i H - \sin \lambda_i CH \right] / \lambda_i \end{array} \right\} \tag{A5}$$

$$M_Z(0) = \sum_{i=1}^{+\infty} A_i \left\{ \begin{array}{l} e^{-\gamma_i CH} M_i(0) - M_i(CH) + \\ CH \left[\begin{array}{l} (\lambda_i \sin \lambda_i CH + \gamma_i \cos \lambda_i CH) / \alpha_i^+ \\ + (\sin \lambda_i H - \sin \lambda_i CH) / \lambda_i \end{array} \right] \\ + \dfrac{\left[\lambda_i H (1-C) \sin \lambda_i H - \cos \lambda_i CH \right]}{\lambda_i^2} \end{array} \right\}. \tag{A6}$$

with

$$M_i(0) = n_i / \alpha_i^{+2}.$$

3. Graphical representation of the 1st water mode shape of vibration for undamped and damped fluid cases
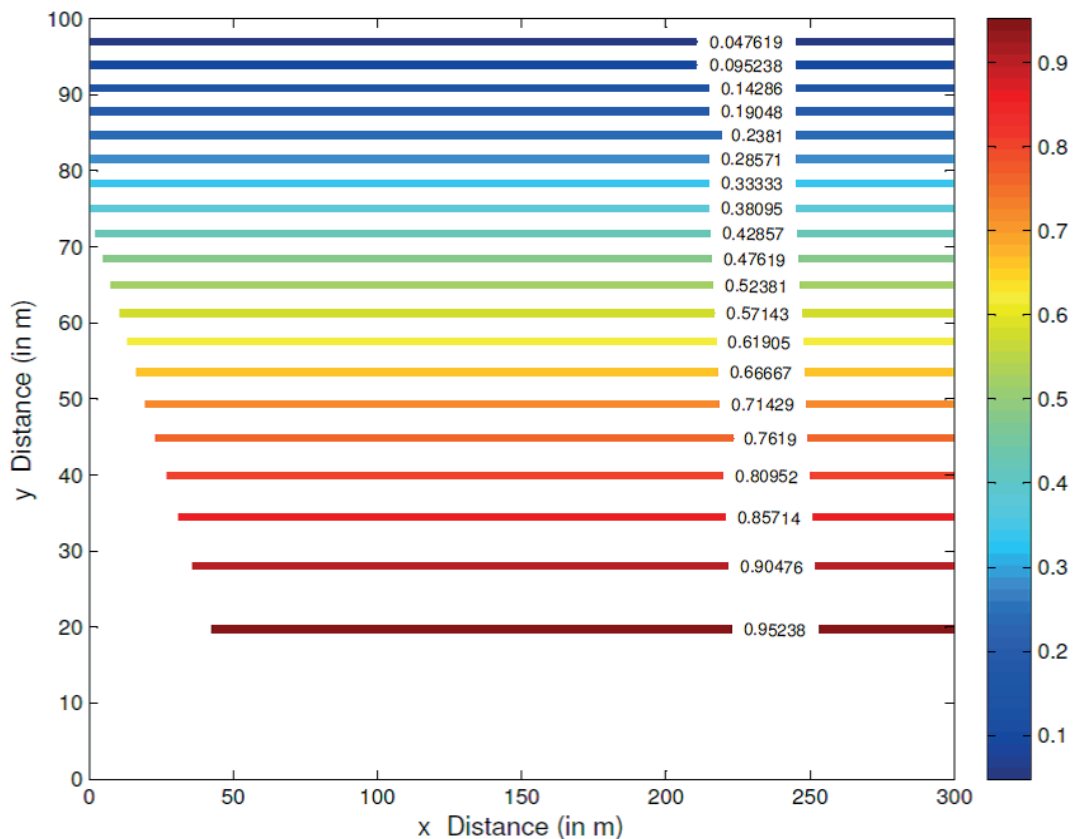
Fig. 1(a) Mode shape of the 1st natural water mode of vibration in the reservoir, $w = w_1 = \dfrac{\pi c}{2H} = 22.588$ rad/sec, $\xi = 0\%$, $T_1(x, y, w_1) = e^{-\mu_1 x} \cos \lambda_1 y$ with $\mu_1 = \sqrt{\lambda_1^2 - K^2}$ and $K = \dfrac{w_1}{c}$
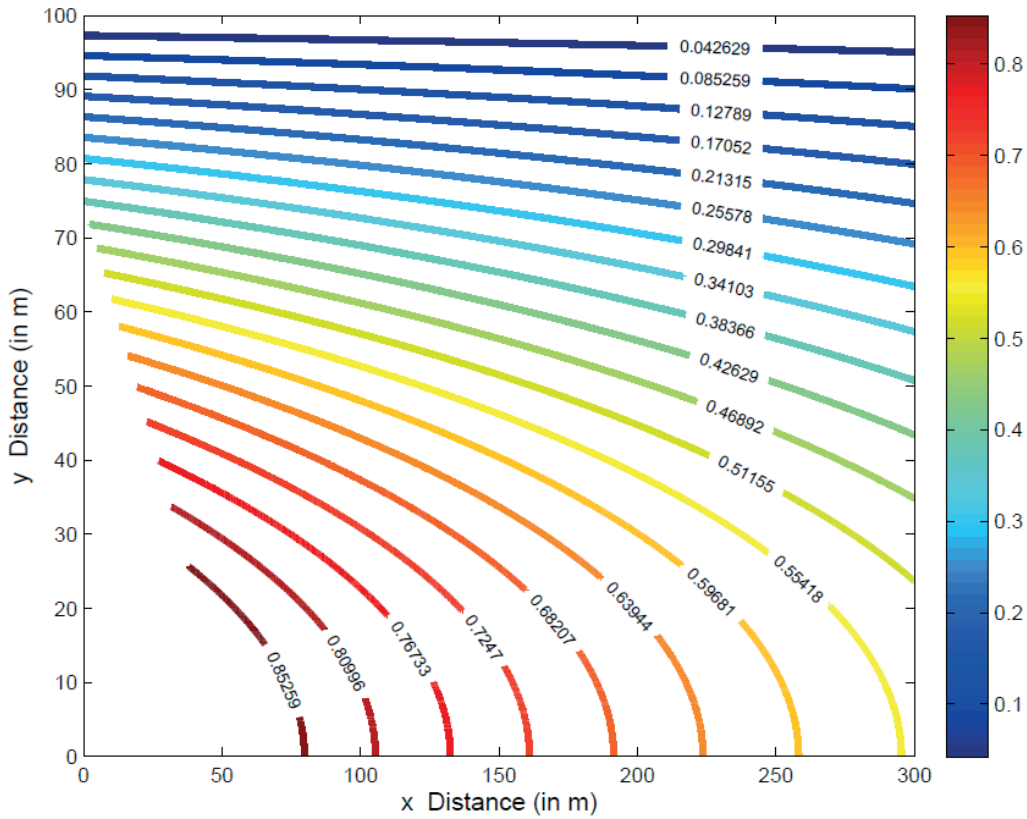
Fig. 1(b) Mode shape of the 1st natural water mode of vibration in the reservoir, $w = w_1 = \dfrac{\pi c}{2H} = 22.588$ rad/sec, $\xi = 1\%$, $T_1(x, y, w_1) = e^{-\mu_1 x} \cos\lambda_1 y$ with $\mu_1 = \sqrt{\lambda_1^2 - K^2}$ and $K = \dfrac{w_1}{c}$. Here c, K and $T_1(x, y, w_1)$ are complex valued.

4. Graphical representation of the 2nd water mode shape of vibration for undamped and damped fluid cases
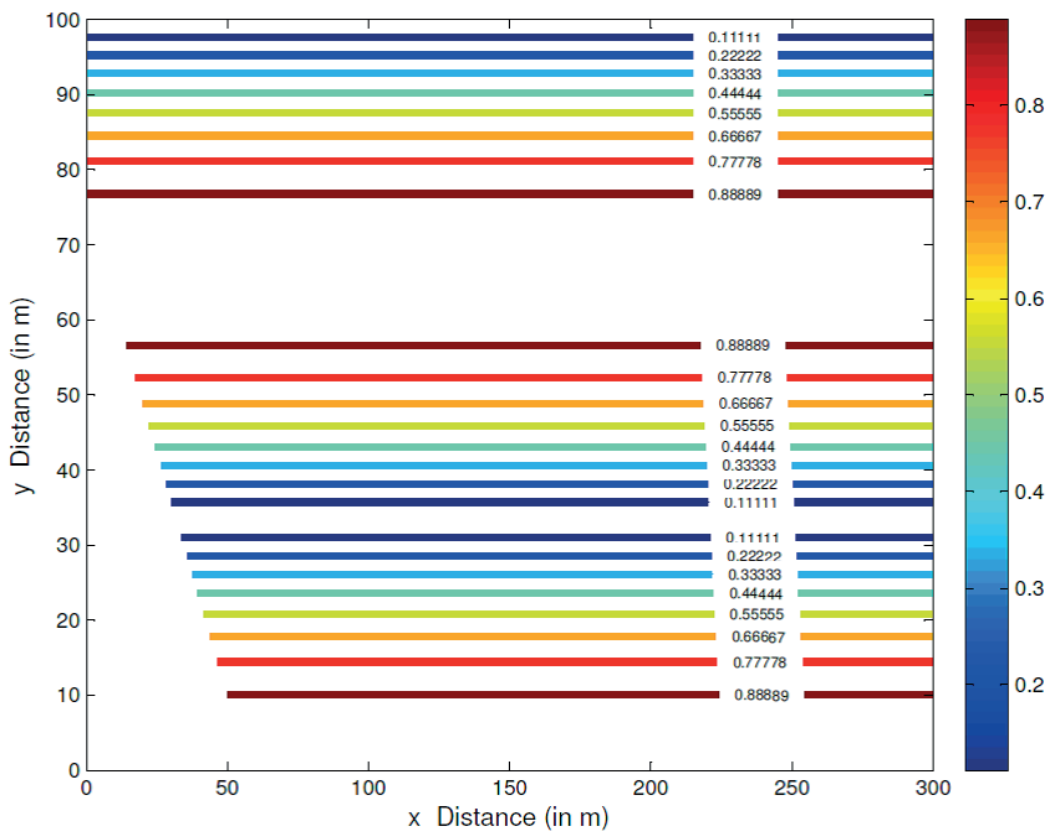
Fig. 2(a) Mode shape of the 2nd natural water mode of vibration in the reservoir, $w = w_2 = \dfrac{3\pi c}{2H} = 67.76$ rad/sec, $\xi = 0\%$, $T_2(x, y, w_2) = e^{-\mu_2 x} \cos\lambda_2 y$ with $\mu_2 = \sqrt{\lambda_2^2 - K^2}$ and $K = \dfrac{w_2}{c}$

Period. Polytech. Civil Eng.

A. Tadjadit, B. Tiliouine
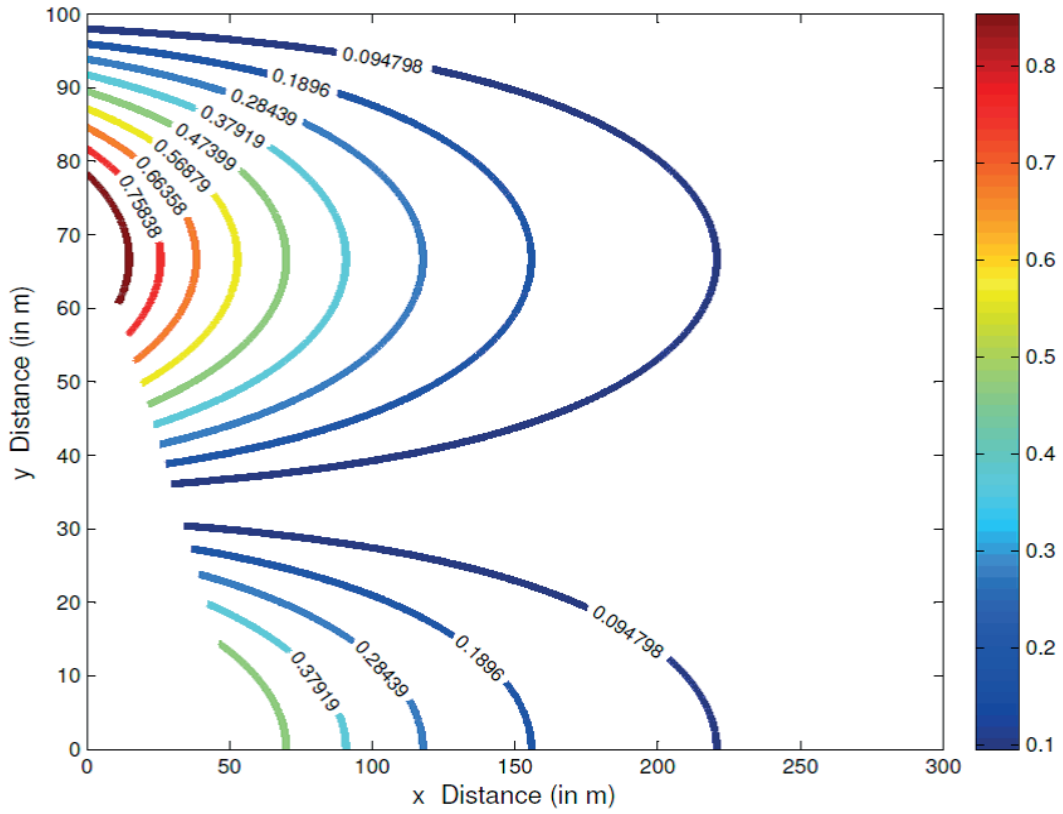
Fig. 2(b) Mode shape of the 2nd natural water mode of vibration in the reservoir, $w = w_2 = \dfrac{3\pi c}{2H} = 67.76 \; rad \,/\, \sec$, $\xi = 1\%$, $T_2(x, y, w_2) = e^{-\mu_2 x} \cos\lambda_2 y$ with $\mu_2 = \sqrt{\lambda_2^2 - K^2}$ and $K = \dfrac{w_2}{c}$. Here c, K and $T_2(x, y, w_2)$ are complex valued.

5. Graphical representation of the 3rd water mode shape of vibration for undamped and damped fluid cases
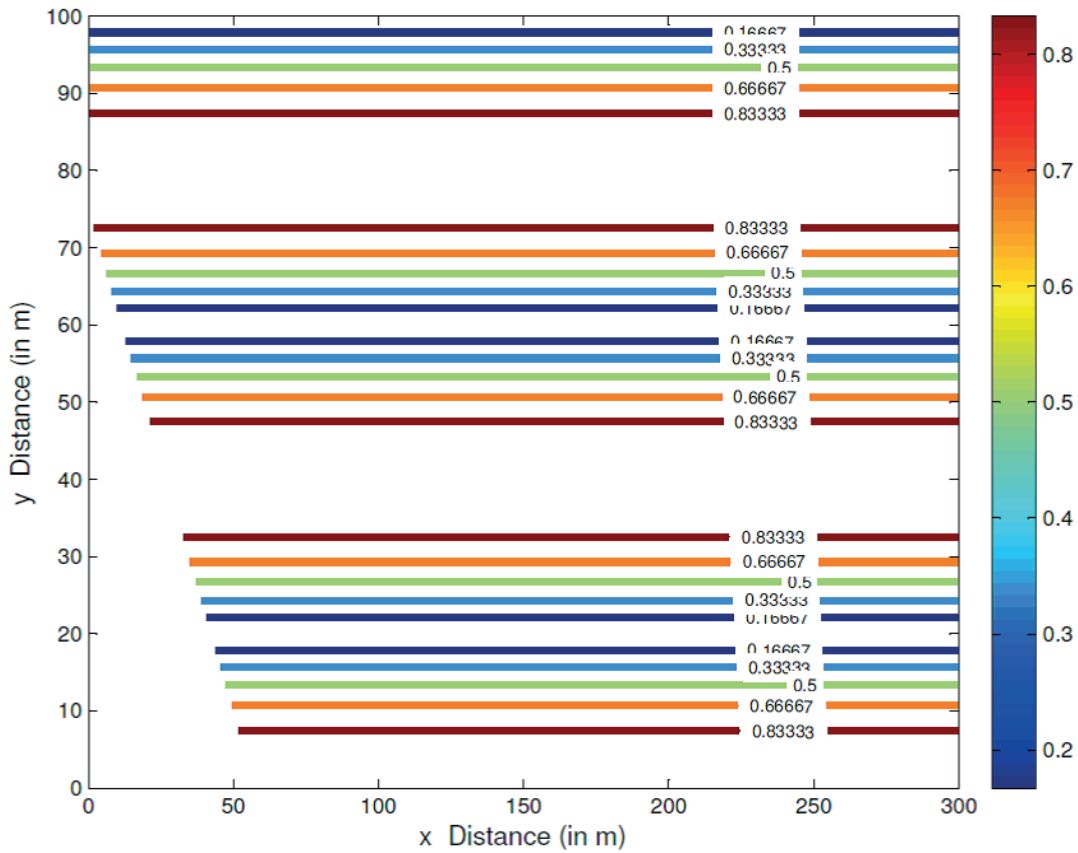
Fig. 3(a) Mode shape of the 3rd natural water mode of vibration in the reservoir, $w = w_3 = \dfrac{5\pi c}{2H} = 112.94 \; rad \,/\, \sec$, $\xi = 0\%$, $T_3(x, y, w_3) = e^{-\mu_3 x} \cos\lambda_3 y$ with $\mu_3 = \sqrt{\lambda_3^2 - K^2}$ and $K = \dfrac{w_3}{c}$.
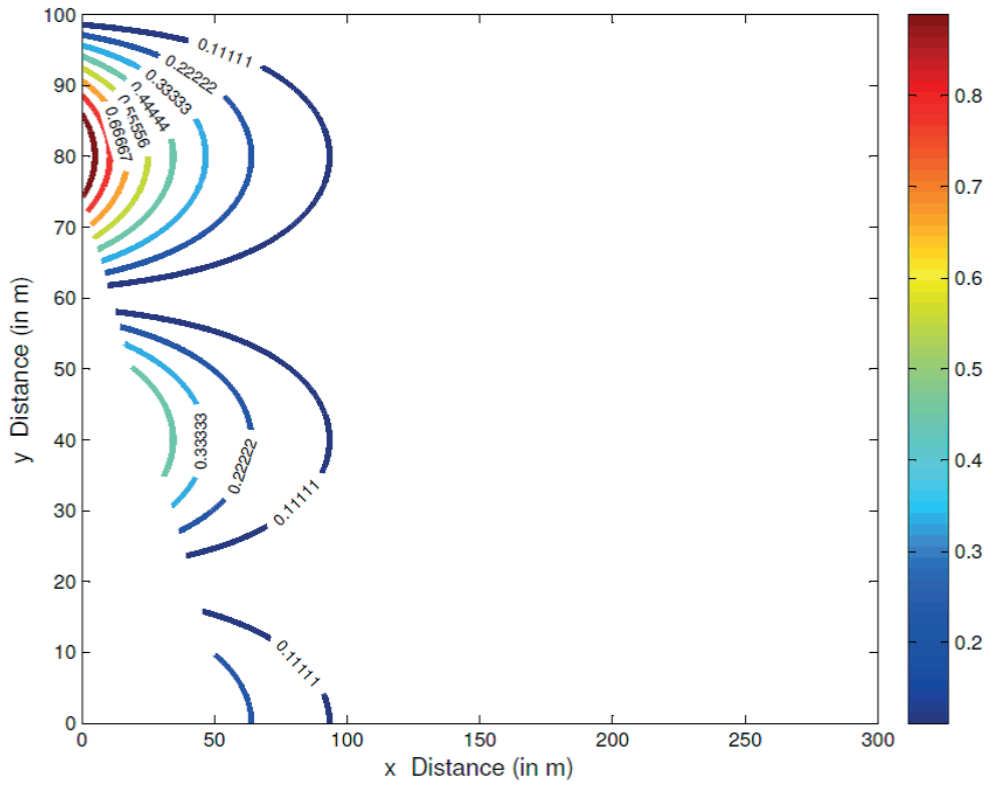
Fig. 3(b) Mode shape of the 3rd natural water mode of vibration in the reservoir, $w = w_3 = \dfrac{5\pi c}{2\mathrm{H}} = 112.94 \; rad/\sec$, $\zeta = 1\%$, $T_3(x, y, w_3) = e^{-\mu_3 x}\cos\lambda_3 y$ with $\mu_3 = \sqrt{\lambda_3^2 - K^2}$ and $K = \dfrac{w_3}{c}$. Here c, K and $T_3(x, y, w_3)$ are complex valued.

Appendix B

We give hereafter the component values of the Hermician matrix $[F_{ji}]$, the column vector $\{G_j\}$ and the column vector of the unknown coefficients $\{A_i\}$ computed using the system of linear equations given by Eq. (14) for calculation of the maximum values of the total shear forces and overturning moments at the base of the dam $F_h(0)$ and $M_z(0)$ (Equations A5 and A6). Twenty five terms have been used to calculate these forces considering an accuracy of 10^{-4} and the following parameters: H = 100m, L = 3H, c = 1438m/s, θ = 37.6°, C = 0.75, C_s = 0.1 and $w = w_1 = \pi c/200$. For reasons of space we consider only the cases of $\zeta = 0\%$ (undamped fluid) and the case of $\zeta = 1\%$ (damped fluid).

a) $[F_{ji}]$, $\{G_j\}$ and $\{A_i\}$ for damping ratio $\zeta = 0\%$ (Inviscid fluid)

Columns 1 through 7

```
 0.0048 + 0.0000i  -0.0067 + 0.0000i  -0.0045 - 0.0000i   0.0125 - 0.0000i  -0.0129 + 0.0000i   0.0056 - 0.0000i   0.0050 - 0.0000i
-0.0067 - 0.0000i   0.0483 + 0.0000i  -0.0403 + 0.0000i   0.0073 - 0.0000i   0.0176 - 0.0000i  -0.0210 + 0.0000i   0.0062 - 0.0000i
-0.0045 + 0.0000i  -0.0403 - 0.0000i   0.1078 + 0.0000i  -0.1200 - 0.0000i   0.0779 - 0.0000i  -0.0168 + 0.0000i  -0.0305 + 0.0000i
 0.0125 + 0.0000i   0.0073 + 0.0000i  -0.1200 - 0.0000i   0.2337 + 0.0000i  -0.2489 + 0.0000i   0.1552 - 0.0000i  -0.0131 + 0.0000i
-0.0129 - 0.0000i   0.0176 + 0.0000i   0.0779 + 0.0000i  -0.2489 - 0.0000i   0.3698 + 0.0000i  -0.3435 + 0.0000i   0.1822 - 0.0000i
 0.0056 + 0.0000i  -0.0210 - 0.0000i  -0.0168 - 0.0000i   0.1552 + 0.0000i  -0.3435 - 0.0000i   0.4609 + 0.0000i  -0.4247 + 0.0000i
 0.0050 + 0.0000i   0.0062 + 0.0000i  -0.0305 - 0.0000i  -0.0131 - 0.0000i   0.1822 + 0.0000i  -0.4247 - 0.0000i   0.6067 + 0.0000i
-0.0128 - 0.0000i   0.0133 + 0.0000i   0.0468 + 0.0000i  -0.0988 + 0.0000i   0.0167 - 0.0000i   0.2534 + 0.0000i  -0.6152 - 0.0000i
 0.0130 + 0.0000i  -0.0233 - 0.0000i  -0.0332 - 0.0000i   0.1289 + 0.0000i  -0.1442 - 0.0000i  -0.0437 - 0.0000i   0.4357 + 0.0000i
-0.0055 - 0.0000i   0.0172 + 0.0000i   0.0039 - 0.0000i  -0.0753 - 0.0000i   0.1458 + 0.0000i  -0.0998 - 0.0000i  -0.1554 - 0.0000i
-0.0052 - 0.0000i   0.0005 - 0.0000i   0.0226 + 0.0000i  -0.0195 + 0.0000i  -0.0452 - 0.0000i   0.1258 + 0.0000i  -0.0954 - 0.0000i
 0.0129 + 0.0000i  -0.0182 - 0.0000i  -0.0327 - 0.0000i   0.0955 - 0.0000i  -0.0788 + 0.0000i  -0.0561 - 0.0000i   0.2165 + 0.0000i
-0.0130 - 0.0000i   0.0245 + 0.0000i   0.0232 - 0.0000i  -0.1094 - 0.0000i   0.1440 + 0.0000i  -0.0397 + 0.0000i  -0.1843 - 0.0000i
 0.0055 + 0.0000i  -0.0155 - 0.0000i  -0.0020 + 0.0000i   0.0570 + 0.0000i  -0.1125 - 0.0000i   0.0923 + 0.0000i   0.0526 + 0.0000i
 0.0052 + 0.0000i  -0.0034 + 0.0000i  -0.0182 - 0.0000i   0.0273 - 0.0000i   0.0093 + 0.0000i  -0.0729 - 0.0000i   0.0862 + 0.0000i
-0.0129 - 0.0000i   0.0204 + 0.0000i   0.0263 - 0.0000i  -0.0925 - 0.0000i   0.0978 - 0.0000i   0.0034 + 0.0000i  -0.1537 - 0.0000i
 0.0130 + 0.0000i  -0.0251 - 0.0000i  -0.0190 + 0.0000i   0.1009 + 0.0000i  -0.1418 - 0.0000i   0.0642 + 0.0000i   0.1231 + 0.0000i
-0.0055 - 0.0000i   0.0144 + 0.0000i   0.0017 - 0.0000i  -0.0493 - 0.0000i   0.0969 + 0.0000i  -0.0844 - 0.0000i  -0.0253 - 0.0000i
-0.0053 - 0.0000i   0.0050 - 0.0000i   0.0154 + 0.0000i  -0.0303 + 0.0000i   0.0077 - 0.0000i   0.0463 + 0.0000i  -0.0760 - 0.0000i
 0.0129 + 0.0000i  -0.0216 - 0.0000i  -0.0227 + 0.0000i   0.0904 - 0.0000i  -0.1068 + 0.0000i   0.0224 - 0.0000i   0.1229 + 0.0000i
-0.0130 - 0.0000i   0.0253 + 0.0000i   0.0168 - 0.0000i  -0.0962 - 0.0000i   0.1400 + 0.0000i  -0.0752 - 0.0000i  -0.0945 - 0.0000i
 0.0055 + 0.0000i  -0.0138 - 0.0000i  -0.0018 + 0.0000i   0.0452 + 0.0000i  -0.0877 - 0.0000i   0.0781 + 0.0000i   0.0143 - 0.0000i
 0.0053 + 0.0000i  -0.0061 - 0.0000i  -0.0135 - 0.0000i   0.0317 - 0.0000i  -0.0176 + 0.0000i  -0.0298 - 0.0000i   0.0674 + 0.0000i
-0.0129 - 0.0000i   0.0224 + 0.0000i   0.0204 - 0.0000i  -0.0889 + 0.0000i   0.1119 - 0.0000i  -0.0377 + 0.0000i  -0.1040 - 0.0000i
 0.0130 + 0.0000i  -0.0255 - 0.0000i  -0.0154 + 0.0000i   0.0933 + 0.0000i  -0.1385 - 0.0000i   0.0813 + 0.0000i   0.0781 - 0.0000i
```

Columns 8 through 14

```
-0.0128 + 0.0000i    0.0130 - 0.0000i   -0.0055 + 0.0000i   -0.0052 + 0.0000i    0.0129 - 0.0000i   -0.0130 + 0.0000i    0.0055 - 0.0000i
 0.0133 - 0.0000i   -0.0233 + 0.0000i    0.0172 - 0.0000i    0.0005 + 0.0000i   -0.0182 + 0.0000i    0.0245 - 0.0000i   -0.0155 + 0.0000i
 0.0468 - 0.0000i   -0.0332 + 0.0000i    0.0039 + 0.0000i    0.0226 - 0.0000i   -0.0327 + 0.0000i    0.0232 + 0.0000i   -0.0020 - 0.0000i
-0.0988 - 0.0000i    0.1289 - 0.0000i   -0.0753 + 0.0000i   -0.0195 - 0.0000i    0.0955 + 0.0000i   -0.1094 + 0.0000i    0.0570 - 0.0000i
 0.0167 + 0.0000i   -0.1442 + 0.0000i    0.1458 - 0.0000i   -0.0452 + 0.0000i   -0.0788 - 0.0000i    0.1440 - 0.0000i   -0.1125 + 0.0000i
 0.2534 - 0.0000i   -0.0437 + 0.0000i   -0.0998 + 0.0000i    0.1258 - 0.0000i   -0.0561 + 0.0000i   -0.0397 - 0.0000i    0.0923 - 0.0000i
-0.6152 + 0.0000i    0.4357 - 0.0000i   -0.1554 + 0.0000i   -0.0954 + 0.0000i    0.2165 - 0.0000i   -0.1843 + 0.0000i    0.0526 - 0.0000i
 0.8743 + 0.0000i   -0.8717 + 0.0000i    0.5894 - 0.0000i   -0.1612 + 0.0000i   -0.2090 - 0.0000i    0.3623 - 0.0000i   -0.2660 + 0.0000i
-0.8717 - 0.0000i    1.1208 + 0.0000i   -1.0326 + 0.0000i    0.6360 - 0.0000i   -0.1232 + 0.0000i   -0.2648 + 0.0000i    0.3738 - 0.0000i
 0.5894 + 0.0000i   -1.0326 - 0.0000i    1.2675 + 0.0000i   -1.1636 + 0.0000i    0.7587 - 0.0000i   -0.2379 + 0.0000i   -0.1735 + 0.0000i
-0.1612 - 0.0000i    0.6360 + 0.0000i   -1.1636 - 0.0000i    1.5003 + 0.0000i   -1.4651 + 0.0000i    1.0479 - 0.0000i   -0.4202 + 0.0000i
-0.2090 + 0.0000i   -0.1232 - 0.0000i    0.7587 + 0.0000i   -1.4651 - 0.0000i    1.9097 + 0.0000i   -1.8492 + 0.0000i    1.2763 - 0.0000i
 0.3623 + 0.0000i   -0.2648 - 0.0000i   -0.2379 - 0.0000i    1.0479 + 0.0000i   -1.8492 - 0.0000i    2.2666 + 0.0000i   -2.0766 + 0.0000i
-0.2660 - 0.0000i    0.3738 + 0.0000i   -0.1735 - 0.0000i   -0.4202 - 0.0000i    1.2763 + 0.0000i   -2.0766 - 0.0000i    2.4688 + 0.0000i
 0.0195 + 0.0000i   -0.2129 - 0.0000i    0.3308 + 0.0000i   -0.1559 - 0.0000i   -0.4337 - 0.0000i    1.3423 + 0.0000i   -2.2575 - 0.0000i
 0.2120 - 0.0000i   -0.0671 + 0.0000i   -0.2355 - 0.0000i    0.4634 + 0.0000i   -0.3132 - 0.0000i   -0.3865 - 0.0000i    1.5163 + 0.0000i
-0.2932 - 0.0000i    0.2730 + 0.0000i    0.0133 + 0.0000i   -0.4335 - 0.0000i    0.6677 + 0.0000i   -0.3801 - 0.0000i   -0.5540 - 0.0000i
 0.1897 + 0.0000i   -0.2827 - 0.0000i    0.1713 + 0.0000i    0.1634 + 0.0000i   -0.5500 - 0.0000i    0.6736 + 0.0000i   -0.2438 - 0.0000i
 0.0223 - 0.0000i    0.1073 + 0.0000i   -0.2109 - 0.0000i    0.1516 + 0.0000i    0.1209 + 0.0000i   -0.4735 - 0.0000i    0.6083 - 0.0000i
-0.2093 + 0.0000i    0.1290 - 0.0000i    0.1053 + 0.0000i   -0.3292 - 0.0000i    0.3238 + 0.0000i    0.0076 + 0.0000i   -0.5060 - 0.0000i
 0.2614 + 0.0000i   -0.2735 - 0.0000i    0.0568 - 0.0000i    0.2911 + 0.0000i   -0.5228 - 0.0000i    0.3962 + 0.0000i    0.1261 + 0.0000i
-0.1543 - 0.0000i    0.2396 + 0.0000i   -0.1636 - 0.0000i   -0.0888 - 0.0000i    0.3860 + 0.0000i   -0.4984 - 0.0000i    0.2471 + 0.0000i
-0.0413 + 0.0000i   -0.0552 - 0.0000i    0.1519 + 0.0000i   -0.1419 - 0.0000i   -0.0260 - 0.0000i    0.2705 + 0.0000i   -0.3951 - 0.0000i
 0.2057 - 0.0000i   -0.1600 + 0.0000i   -0.0402 - 0.0000i    0.2657 + 0.0000i   -0.3252 - 0.0000i    0.1138 - 0.0000i    0.2705 + 0.0000i
-0.2426 - 0.0000i    0.2718 + 0.0000i   -0.0910 - 0.0000i   -0.2231 - 0.0000i    0.4588 + 0.0000i   -0.4017 - 0.0000i    0.0064 - 0.0000i
```

Columns 15 through 21

```
 0.0052 - 0.0000i   -0.0129 + 0.0000i    0.0130 - 0.0000i   -0.0055 + 0.0000i   -0.0053 + 0.0000i    0.0129 - 0.0000i   -0.0130 + 0.0000i
-0.0034 - 0.0000i    0.0204 - 0.0000i   -0.0251 + 0.0000i    0.0144 - 0.0000i    0.0050 + 0.0000i   -0.0216 + 0.0000i    0.0253 - 0.0000i
-0.0182 - 0.0000i    0.0263 + 0.0000i   -0.0190 - 0.0000i    0.0017 + 0.0000i    0.0154 - 0.0000i   -0.0227 + 0.0000i    0.0168 + 0.0000i
 0.0273 + 0.0000i   -0.0925 - 0.0000i    0.1009 + 0.0000i   -0.0493 + 0.0000i   -0.0303 - 0.0000i    0.0904 + 0.0000i   -0.0962 + 0.0000i
 0.0093 - 0.0000i    0.0978 + 0.0000i   -0.1418 + 0.0000i    0.0969 - 0.0000i    0.0077 + 0.0000i   -0.1068 - 0.0000i    0.1400 - 0.0000i
-0.0729 + 0.0000i    0.0034 - 0.0000i    0.0642 - 0.0000i   -0.0844 + 0.0000i    0.0463 - 0.0000i    0.0224 + 0.0000i   -0.0752 + 0.0000i
 0.0862 - 0.0000i   -0.1537 + 0.0000i    0.1231 - 0.0000i   -0.0253 - 0.0000i   -0.0760 + 0.0000i    0.1229 - 0.0000i   -0.0945 + 0.0000i
 0.0195 + 0.0000i    0.2120 + 0.0000i   -0.2932 - 0.0000i    0.1897 - 0.0000i    0.0223 + 0.0000i   -0.2093 + 0.0000i    0.2614 + 0.0000i
-0.2129 + 0.0000i   -0.0671 - 0.0000i    0.2730 - 0.0000i   -0.2827 + 0.0000i    0.1073 - 0.0000i    0.1290 + 0.0000i   -0.2735 + 0.0000i
 0.3308 - 0.0000i   -0.2355 + 0.0000i    0.0133 - 0.0000i    0.1713 - 0.0000i   -0.2109 + 0.0000i    0.1053 - 0.0000i    0.0568 + 0.0000i
-0.1559 + 0.0000i    0.4634 - 0.0000i   -0.4335 + 0.0000i    0.1634 - 0.0000i    0.1516 - 0.0000i   -0.3292 + 0.0000i    0.2911 - 0.0000i
-0.4337 + 0.0000i   -0.3132 - 0.0000i    0.6677 - 0.0000i   -0.5500 + 0.0000i    0.1209 - 0.0000i    0.3238 + 0.0000i   -0.5228 + 0.0000i
 1.3423 - 0.0000i   -0.3865 + 0.0000i   -0.3801 - 0.0000i    0.6736 - 0.0000i   -0.4735 + 0.0000i    0.0076 + 0.0000i    0.3962 - 0.0000i
-2.2575 + 0.0000i    1.5163 - 0.0000i   -0.5540 + 0.0000i   -0.2438 - 0.0000i    0.6083 + 0.0000i   -0.5060 + 0.0000i    0.1261 - 0.0000i
 2.7887 + 0.0000i   -2.6702 + 0.0000i    1.9117 - 0.0000i   -0.8055 + 0.0000i   -0.2138 + 0.0000i    0.7816 - 0.0000i   -0.7707 + 0.0000i
-2.6702 - 0.0000i    3.3399 + 0.0000i   -3.1820 + 0.0000i    2.2148 - 0.0000i   -0.8264 - 0.0000i   -0.4146 - 0.0000i    1.0433 - 0.0000i
 1.9117 + 0.0000i   -3.1820 - 0.0000i    3.8071 + 0.0000i   -3.4759 + 0.0000i    2.3002 - 0.0000i   -0.7699 + 0.0000i   -0.4930 + 0.0000i
-0.8055 - 0.0000i    2.2148 + 0.0000i   -3.4759 - 0.0000i    4.0649 + 0.0000i   -3.7069 + 0.0000i    2.5253 - 0.0000i   -0.9898 + 0.0000i
-0.2138 - 0.0000i   -0.8264 - 0.0000i    2.3002 + 0.0000i   -3.7069 - 0.0000i    4.4718 + 0.0000i   -4.2306 + 0.0000i    3.0269 + 0.0000i
 0.7816 + 0.0000i   -0.4146 + 0.0000i   -0.7699 - 0.0000i    2.5253 + 0.0000i   -4.2306 - 0.0000i    5.1648 + 0.0000i   -4.8701 + 0.0000i
-0.7707 - 0.0000i    1.0433 + 0.0000i   -0.4930 - 0.0000i   -0.9898 - 0.0000i    3.0269 + 0.0000i   -4.8701 - 0.0000i    5.7424 + 0.0000i
 0.3309 + 0.0000i   -0.9208 - 0.0000i    1.0440 + 0.0000i   -0.3126 - 0.0000i   -1.3101 - 0.0000i    3.4045 + 0.0000i   -5.2305 - 0.0000i
 0.2143 + 0.0000i    0.2788 + 0.0000i   -0.8212 - 0.0000i    0.9568 + 0.0000i   -0.2706 - 0.0000i   -1.3383 + 0.0000i    3.5096 + 0.0000i
-0.5478 - 0.0000i    0.4313 - 0.0000i    0.1388 + 0.0000i   -0.8630 - 0.0000i    1.1704 + 0.0000i   -0.5148 + 0.0000i   -1.2726 - 0.0000i
 0.5175 + 0.0000i   -0.7929 - 0.0000i    0.5151 + 0.0000i    0.2939 + 0.0000i   -1.1933 - 0.0000i    1.4892 + 0.0000i   -0.6047 - 0.0000i
```

Columns 22 through 25

```
 0.0055 - 0.0000i    0.0053 - 0.0000i   -0.0129 + 0.0000i    0.0130 - 0.0000i
-0.0138 + 0.0000i   -0.0061 + 0.0000i    0.0224 - 0.0000i   -0.0255 + 0.0000i
-0.0018 - 0.0000i   -0.0135 - 0.0000i    0.0204 - 0.0000i   -0.0154 - 0.0000i
 0.0452 - 0.0000i    0.0317 - 0.0000i   -0.0889 - 0.0000i    0.0933 - 0.0000i
-0.0877 + 0.0000i   -0.0176 - 0.0000i    0.1119 + 0.0000i   -0.1385 + 0.0000i
 0.0781 - 0.0000i   -0.0298 + 0.0000i   -0.0377 - 0.0000i    0.0813 - 0.0000i
 0.0143 + 0.0000i    0.0674 - 0.0000i   -0.1040 + 0.0000i    0.0781 + 0.0000i
-0.1543 - 0.0000i   -0.0413 - 0.0000i    0.2057 + 0.0000i   -0.2426 + 0.0000i
 0.2396 - 0.0000i   -0.0552 + 0.0000i   -0.1600 + 0.0000i    0.2718 - 0.0000i
-0.1636 + 0.0000i    0.1519 - 0.0000i   -0.0402 + 0.0000i   -0.0910 + 0.0000i
-0.0888 + 0.0000i   -0.1419 + 0.0000i    0.2657 - 0.0000i   -0.2231 + 0.0000i
 0.3860 - 0.0000i   -0.0260 + 0.0000i   -0.3252 - 0.0000i    0.4588 - 0.0000i
-0.4984 + 0.0000i    0.2705 - 0.0000i    0.1138 + 0.0000i   -0.4017 + 0.0000i
 0.2471 - 0.0000i   -0.3951 - 0.0000i    0.2705 - 0.0000i    0.0064 - 0.0000i
 0.3309 - 0.0000i    0.2143 - 0.0000i   -0.5478 - 0.0000i    0.5175 - 0.0000i
-0.9208 + 0.0000i    0.2788 - 0.0000i    0.4313 + 0.0000i   -0.7929 + 0.0000i
 1.0440 - 0.0000i   -0.8212 + 0.0000i    0.1388 - 0.0000i    0.5151 - 0.0000i
-0.3126 + 0.0000i    0.9568 - 0.0000i   -0.8630 - 0.0000i    0.2939 - 0.0000i
-1.3101 + 0.0000i   -0.2706 + 0.0000i    1.1704 - 0.0000i   -1.1933 + 0.0000i
 3.4045 + 0.0000i   -1.3383 - 0.0000i   -0.5148 + 0.0000i    1.4892 - 0.0000i
-5.2305 + 0.0000i    3.5096 - 0.0000i   -1.2726 + 0.0000i   -0.6047 + 0.0000i
 6.0557 + 0.0000i   -5.5116 + 0.0000i    3.7858 - 0.0000i   -1.5446 + 0.0000i
-5.5116 - 0.0000i    6.5497 + 0.0000i   -6.1465 + 0.0000i    4.3936 - 0.0000i
 3.7858 + 0.0000i   -6.1465 - 0.0000i    7.3846 + 0.0000i   -6.9136 + 0.0000i
-1.5446 - 0.0000i    4.3936 + 0.0000i   -6.9136 - 0.0000i    8.0725 + 0.0000i
```

$\{G_j\}^T = $ 1.0e+03*{0.5886 - 0.0000i -0.9675 + 0.0000i 0.8356 - 0.0000i -0.7224 + 0.0000i 0.7364 - 0.0000i -0.8821 + 0.0000i 1.0805 + 0.0000i   -1.2188 - 0.0000i 1.2172 - 0.0000i -1.0769 + 0.0000i 0.8799 - 0.0000i -0.7415 + 0.0000i 0.7425 - 0.0000i -0.8825 + 0.0000i 1.0796 + 0.0000i -1.2187 - 0.0000i 1.2182 - 0.0000i   -1.0787 + 0.0000i 0.8817 - 0.0000i -0.7427 + 0.0000i 0.7431 - 0.0000i -0.8825 + 0.0000i 1.0795 + 0.0000i -1.2186 - 0.0000i 0.0000 + 0.0000i}.

$\{A_i\}^T = $ 1.0e+09*{0.0002 - 0.0000i 0.0001 - 0.0000i 0.0001 - 0.0000i 0.0002 - 0.0000i 0.0006 - 0.0000i 0.0017 - 0.0000i 0.0048 - 0.0000i 0.0127 - 0.0000i   0.0319 - 0.0000i 0.0747 - 0.0000i 0.1617 - 0.0000i 0.3196 - 0.0000i 0.5715 - 0.0000i 0.9164 - 0.0000i 1.3059 - 0.0000i 1.6382 - 0.0000i 1.7899 - 0.0000i 1.6827 - 0.0000i 1.3406 - 0.0000i 0.8877 - 0.0000i 0.4758 - 0.0000i 0.1986 - 0.0000i 0.0607 - 0.0000i 0.0121 - 0.0000i 0.0012 - 0.0000i}.

b) $[F_{ji}]$, $\{G_j\}$ and $\{A_i\}$ for damping ratio $\xi = 1\%$

```
Columns 1 through 7

 0.0065 + 0.0000i  -0.0071 + 0.0004i  -0.0043 - 0.0001i   0.0126 - 0.0001i  -0.0132 + 0.0003i   0.0058 - 0.0002i   0.0050 + 0.0000i
-0.0071 - 0.0004i   0.0483 + 0.0000i  -0.0403 + 0.0000i   0.0073 - 0.0000i   0.0176 - 0.0000i  -0.0210 + 0.0000i   0.0062 - 0.0000i
-0.0043 + 0.0001i  -0.0403 - 0.0000i   0.1078 + 0.0000i  -0.1200 + 0.0000i   0.0779 - 0.0000i  -0.0168 + 0.0000i  -0.0305 + 0.0000i
 0.0126 + 0.0001i   0.0073 + 0.0000i  -0.1200 - 0.0000i   0.2337 + 0.0000i  -0.2489 + 0.0000i   0.1552 - 0.0000i  -0.0131 + 0.0000i
-0.0132 - 0.0003i   0.0176 + 0.0000i   0.0779 + 0.0000i  -0.2489 - 0.0000i   0.3698 + 0.0000i  -0.3435 + 0.0000i   0.1822 - 0.0000i
 0.0058 + 0.0002i  -0.0210 - 0.0000i  -0.0168 - 0.0000i   0.1552 - 0.0000i  -0.3435 - 0.0000i   0.4609 + 0.0000i  -0.4247 + 0.0000i
 0.0050 - 0.0000i   0.0062 + 0.0000i  -0.0305 - 0.0000i  -0.0131 - 0.0000i   0.1822 + 0.0000i  -0.4247 - 0.0000i   0.6068 + 0.0000i
-0.0129 - 0.0002i   0.0133 + 0.0000i   0.0468 + 0.0000i  -0.0988 + 0.0000i   0.0167 - 0.0000i   0.2534 + 0.0000i  -0.6152 - 0.0000i
 0.0132 + 0.0002i  -0.0233 - 0.0000i  -0.0332 - 0.0000i   0.1289 + 0.0000i  -0.1442 - 0.0000i  -0.0437 - 0.0000i   0.4357 + 0.0000i
-0.0057 - 0.0001i   0.0172 + 0.0000i   0.0039 - 0.0000i  -0.0753 - 0.0000i   0.1458 + 0.0000i  -0.0998 - 0.0000i  -0.1554 - 0.0000i
-0.0052 - 0.0000i   0.0005 - 0.0000i   0.0226 + 0.0000i  -0.0195 + 0.0000i  -0.0452 - 0.0000i   0.1258 + 0.0000i  -0.0954 - 0.0000i
 0.0130 + 0.0002i  -0.0182 - 0.0000i  -0.0327 - 0.0000i   0.0955 + 0.0000i  -0.0788 - 0.0000i  -0.0561 - 0.0000i   0.2165 + 0.0000i
-0.0132 - 0.0002i   0.0245 + 0.0000i   0.0232 - 0.0000i  -0.1094 - 0.0000i   0.1440 + 0.0000i  -0.0397 - 0.0000i  -0.1843 - 0.0000i
 0.0056 + 0.0001i  -0.0155 - 0.0000i  -0.0020 + 0.0000i   0.0570 + 0.0000i  -0.1125 - 0.0000i   0.0923 + 0.0000i   0.0526 + 0.0000i
 0.0053 + 0.0000i  -0.0034 - 0.0000i  -0.0182 - 0.0000i   0.0273 - 0.0000i   0.0093 + 0.0000i  -0.0729 - 0.0000i   0.0862 + 0.0000i
-0.0131 - 0.0002i   0.0204 + 0.0000i   0.0263 - 0.0000i  -0.0925 - 0.0000i   0.0978 - 0.0000i   0.0034 + 0.0000i  -0.1537 - 0.0000i
 0.0132 + 0.0002i  -0.0251 - 0.0000i  -0.0190 + 0.0000i   0.1009 + 0.0000i  -0.1418 - 0.0000i   0.0642 + 0.0000i   0.1231 + 0.0000i
-0.0056 - 0.0001i   0.0144 + 0.0000i   0.0017 - 0.0000i  -0.0493 - 0.0000i   0.0969 + 0.0000i  -0.0844 - 0.0000i  -0.0253 + 0.0000i
-0.0053 - 0.0000i   0.0050 - 0.0000i   0.0154 + 0.0000i  -0.0303 - 0.0000i   0.0077 - 0.0000i   0.0463 + 0.0000i  -0.0760 - 0.0000i
 0.0131 + 0.0002i  -0.0216 - 0.0000i  -0.0227 + 0.0000i   0.0904 - 0.0000i  -0.1068 - 0.0000i   0.0224 - 0.0000i   0.1229 + 0.0000i
-0.0132 - 0.0002i   0.0253 + 0.0000i   0.0168 - 0.0000i  -0.0962 - 0.0000i   0.1400 + 0.0000i  -0.0752 - 0.0000i  -0.0945 - 0.0000i
 0.0056 + 0.0001i  -0.0138 - 0.0000i  -0.0018 + 0.0000i   0.0452 + 0.0000i  -0.0877 - 0.0000i   0.0781 + 0.0000i   0.0143 - 0.0000i
 0.0054 + 0.0001i  -0.0061 - 0.0000i  -0.0135 - 0.0000i   0.0317 - 0.0000i  -0.0176 + 0.0000i  -0.0298 - 0.0000i   0.0674 + 0.0000i
-0.0131 - 0.0002i   0.0224 + 0.0000i   0.0204 - 0.0000i  -0.0889 - 0.0000i   0.1119 - 0.0000i  -0.0377 + 0.0000i  -0.1040 - 0.0000i
 0.0132 + 0.0002i  -0.0255 - 0.0000i  -0.0154 + 0.0000i   0.0933 + 0.0000i  -0.1385 - 0.0000i   0.0813 + 0.0000i   0.0781 - 0.0000i


Columns 8 through 14

-0.0129 + 0.0002i   0.0132 - 0.0002i  -0.0057 + 0.0001i  -0.0052 + 0.0000i   0.0130 - 0.0002i  -0.0132 + 0.0002i   0.0056 - 0.0001i
 0.0133 - 0.0000i  -0.0233 + 0.0000i   0.0172 - 0.0000i   0.0005 + 0.0000i  -0.0182 - 0.0000i   0.0245 - 0.0000i  -0.0155 + 0.0000i
 0.0468 - 0.0000i  -0.0332 - 0.0000i   0.0039 - 0.0000i   0.0226 - 0.0000i  -0.0327 - 0.0000i   0.0232 + 0.0000i  -0.0020 - 0.0000i
-0.0988 - 0.0000i   0.1289 - 0.0000i  -0.0753 + 0.0000i  -0.0195 - 0.0000i   0.0955 + 0.0000i  -0.1094 + 0.0000i   0.0570 - 0.0000i
 0.0167 + 0.0000i  -0.1442 + 0.0000i   0.1458 - 0.0000i  -0.0452 + 0.0000i  -0.0788 - 0.0000i   0.1440 - 0.0000i  -0.1125 + 0.0000i
 0.2534 - 0.0000i  -0.0437 + 0.0000i  -0.0998 + 0.0000i   0.1258 - 0.0000i  -0.0561 + 0.0000i  -0.0397 - 0.0000i   0.0923 + 0.0000i
-0.6152 + 0.0000i   0.4357 - 0.0000i  -0.1554 - 0.0000i  -0.0954 - 0.0000i   0.2165 - 0.0000i  -0.1843 + 0.0000i   0.0526 - 0.0000i
 0.8743 + 0.0000i  -0.8717 + 0.0000i   0.5894 - 0.0000i  -0.1612 + 0.0000i  -0.2090 - 0.0000i   0.3623 - 0.0000i  -0.2660 + 0.0000i
-0.8717 - 0.0000i   1.1208 + 0.0000i  -1.0326 + 0.0000i   0.6360 - 0.0000i  -0.1232 + 0.0000i  -0.2648 + 0.0000i   0.3738 - 0.0000i
 0.5894 + 0.0000i  -1.0326 - 0.0000i   1.2675 + 0.0000i  -1.1636 + 0.0000i   0.7587 - 0.0000i  -0.2379 + 0.0000i  -0.1735 + 0.0000i
-0.1612 - 0.0000i   0.6360 + 0.0000i  -1.1636 - 0.0000i   1.5003 + 0.0000i  -1.4651 + 0.0000i   1.0479 - 0.0000i  -0.4202 + 0.0000i
-0.2090 + 0.0000i  -0.1232 - 0.0000i   0.7587 + 0.0000i  -1.4651 - 0.0000i   1.9097 + 0.0000i  -1.8492 + 0.0000i   1.2763 - 0.0000i
 0.3623 - 0.0000i  -0.2648 - 0.0000i  -0.2379 + 0.0000i   1.0479 + 0.0000i  -1.8492 - 0.0000i   2.2666 + 0.0000i  -2.0766 - 0.0000i
-0.2660 - 0.0000i   0.3738 + 0.0000i  -0.1735 - 0.0000i  -0.4202 - 0.0000i   1.2763 + 0.0000i  -2.0766 - 0.0000i   2.4688 + 0.0000i
 0.0195 + 0.0000i  -0.2129 - 0.0000i   0.3308 + 0.0000i  -0.1559 - 0.0000i  -0.4337 - 0.0000i   1.3423 + 0.0000i  -2.2575 - 0.0000i
 0.2120 - 0.0000i  -0.0671 + 0.0000i  -0.2355 - 0.0000i   0.4634 + 0.0000i  -0.3132 + 0.0000i  -0.3865 - 0.0000i   1.5163 + 0.0000i
-0.2932 - 0.0000i   0.2730 + 0.0000i   0.0133 + 0.0000i  -0.4335 - 0.0000i   0.6677 + 0.0000i  -0.3801 - 0.0000i  -0.5540 - 0.0000i
 0.1897 + 0.0000i  -0.2827 - 0.0000i   0.1713 + 0.0000i   0.1634 + 0.0000i  -0.5500 - 0.0000i   0.6736 + 0.0000i  -0.2438 - 0.0000i
 0.0223 - 0.0000i   0.1073 + 0.0000i  -0.2109 - 0.0000i   0.1516 + 0.0000i   0.1209 + 0.0000i  -0.4735 - 0.0000i   0.6083 + 0.0000i
-0.2093 - 0.0000i   0.1290 - 0.0000i   0.1053 - 0.0000i  -0.3292 - 0.0000i   0.3238 + 0.0000i   0.0076 + 0.0000i  -0.5060 - 0.0000i
 0.2614 - 0.0000i  -0.2735 - 0.0000i   0.0568 - 0.0000i   0.2911 + 0.0000i  -0.5228 - 0.0000i   0.3962 + 0.0000i   0.1261 + 0.0000i
-0.1543 - 0.0000i   0.2396 + 0.0000i  -0.1636 - 0.0000i  -0.0888 - 0.0000i   0.3860 + 0.0000i  -0.4984 - 0.0000i   0.2471 + 0.0000i
-0.0413 + 0.0000i  -0.0552 - 0.0000i   0.1519 + 0.0000i  -0.1419 - 0.0000i  -0.0260 - 0.0000i   0.2705 + 0.0000i  -0.3951 - 0.0000i
 0.2057 - 0.0000i  -0.1600 + 0.0000i  -0.0402 - 0.0000i   0.2657 + 0.0000i  -0.3252 - 0.0000i   0.1138 - 0.0000i   0.2705 + 0.0000i
-0.2426 - 0.0000i   0.2718 + 0.0000i  -0.0910 - 0.0000i  -0.2231 - 0.0000i   0.4588 + 0.0000i  -0.4017 - 0.0000i   0.0064 - 0.0000i
```

```
Columns 15 through 21

  0.0053 - 0.0000i  -0.0131 + 0.0002i   0.0132 - 0.0002i  -0.0056 + 0.0001i  -0.0053 + 0.0000i   0.0131 - 0.0002i  -0.0132 + 0.0002i
 -0.0034 - 0.0000i   0.0204 - 0.0000i  -0.0251 + 0.0000i   0.0144 - 0.0000i   0.0050 + 0.0000i  -0.0216 + 0.0000i   0.0253 - 0.0000i
 -0.0182 + 0.0000i   0.0263 + 0.0000i  -0.0190 - 0.0000i   0.0017 + 0.0000i   0.0154 - 0.0000i  -0.0227 - 0.0000i   0.0168 + 0.0000i
  0.0273 + 0.0000i  -0.0925 - 0.0000i   0.1009 - 0.0000i  -0.0493 - 0.0000i  -0.0303 - 0.0000i   0.0904 - 0.0000i  -0.0962 - 0.0000i
  0.0093 - 0.0000i   0.0978 + 0.0000i  -0.1418 + 0.0000i   0.0969 - 0.0000i   0.0077 + 0.0000i  -0.1068 - 0.0000i   0.1400 - 0.0000i
 -0.0729 + 0.0000i   0.0034 - 0.0000i   0.0642 - 0.0000i  -0.0844 + 0.0000i   0.0463 - 0.0000i   0.0224 + 0.0000i  -0.0752 + 0.0000i
  0.0862 - 0.0000i  -0.1537 + 0.0000i   0.1231 - 0.0000i  -0.0253 - 0.0000i  -0.0760 + 0.0000i   0.1229 - 0.0000i  -0.0945 + 0.0000i
  0.0195 - 0.0000i   0.2120 + 0.0000i  -0.2932 + 0.0000i   0.1897 - 0.0000i   0.0223 + 0.0000i  -0.2093 - 0.0000i   0.2614 - 0.0000i
 -0.2129 + 0.0000i  -0.0671 - 0.0000i   0.2730 - 0.0000i  -0.2827 + 0.0000i   0.1073 - 0.0000i   0.1290 + 0.0000i  -0.2735 + 0.0000i
  0.3308 - 0.0000i  -0.2355 + 0.0000i   0.0133 - 0.0000i   0.1713 - 0.0000i  -0.2109 + 0.0000i   0.1053 - 0.0000i   0.0568 + 0.0000i
 -0.1559 + 0.0000i   0.4634 - 0.0000i  -0.4335 + 0.0000i   0.1634 - 0.0000i   0.1516 - 0.0000i  -0.3292 + 0.0000i   0.2911 - 0.0000i
 -0.4337 + 0.0000i  -0.3132 - 0.0000i   0.6677 - 0.0000i  -0.5500 + 0.0000i   0.1209 - 0.0000i   0.3238 + 0.0000i  -0.5228 + 0.0000i
  1.3423 - 0.0000i  -0.3865 + 0.0000i  -0.3801 + 0.0000i   0.6736 - 0.0000i  -0.4735 + 0.0000i   0.0076 - 0.0000i   0.3962 - 0.0000i
 -2.2575 + 0.0000i   1.5163 - 0.0000i  -0.5540 + 0.0000i  -0.2438 + 0.0000i   0.6083 - 0.0000i  -0.5060 + 0.0000i   0.1261 - 0.0000i
  2.7887 + 0.0000i  -2.6702 + 0.0000i   1.9117 - 0.0000i  -0.8055 + 0.0000i  -0.2138 + 0.0000i   0.7816 - 0.0000i  -0.7707 + 0.0000i
 -2.6702 - 0.0000i   3.3399 + 0.0000i  -3.1820 + 0.0000i   2.2148 - 0.0000i  -0.8264 + 0.0000i  -0.4146 + 0.0000i   1.0433 - 0.0000i
  1.9117 + 0.0000i  -3.1820 - 0.0000i   3.8071 + 0.0000i  -3.4759 + 0.0000i   2.3002 - 0.0000i  -0.7699 + 0.0000i  -0.4930 + 0.0000i
 -0.8055 - 0.0000i   2.2148 + 0.0000i  -3.4759 - 0.0000i   4.0649 + 0.0000i  -3.7069 + 0.0000i   2.5253 - 0.0000i  -0.9898 + 0.0000i
 -0.2138 + 0.0000i  -0.8264 - 0.0000i   2.3002 + 0.0000i  -3.7069 - 0.0000i   4.4718 + 0.0000i  -4.2307 + 0.0000i   3.0269 - 0.0000i
  0.7816 + 0.0000i  -0.4146 + 0.0000i  -0.7699 - 0.0000i   2.5253 + 0.0000i  -4.2307 - 0.0000i   5.1648 + 0.0000i  -4.8701 + 0.0000i
 -0.7707 - 0.0000i   1.0433 + 0.0000i  -0.4930 - 0.0000i  -0.9898 + 0.0000i   3.0269 + 0.0000i  -4.8701 - 0.0000i   5.7424 + 0.0000i
  0.3309 + 0.0000i  -0.9208 - 0.0000i   1.0440 - 0.0000i  -0.3126 - 0.0000i  -1.3101 - 0.0000i   3.4045 + 0.0000i  -5.2305 - 0.0000i
  0.2143 + 0.0000i   0.2788 + 0.0000i  -0.8212 - 0.0000i   0.9568 - 0.0000i  -0.2706 - 0.0000i  -1.3383 - 0.0000i   3.5096 + 0.0000i
 -0.5478 - 0.0000i   0.4313 - 0.0000i   0.1388 - 0.0000i  -0.8630 - 0.0000i   1.1704 + 0.0000i  -0.5148 + 0.0000i  -1.2726 - 0.0000i
  0.5175 + 0.0000i  -0.7929 - 0.0000i   0.5151 + 0.0000i   0.2939 + 0.0000i  -1.1933 - 0.0000i   1.4892 + 0.0000i  -0.6047 - 0.0000i


Columns 22 through 25

  0.0056 - 0.0001i   0.0054 - 0.0001i  -0.0131 + 0.0002i   0.0132 - 0.0002i
 -0.0138 + 0.0000i  -0.0061 + 0.0000i   0.0224 - 0.0000i  -0.0255 + 0.0000i
 -0.0018 - 0.0000i  -0.0135 + 0.0000i   0.0204 + 0.0000i  -0.0154 - 0.0000i
  0.0452 - 0.0000i   0.0317 + 0.0000i  -0.0889 - 0.0000i   0.0933 - 0.0000i
 -0.0877 + 0.0000i  -0.0176 - 0.0000i   0.1119 + 0.0000i  -0.1385 + 0.0000i
  0.0781 - 0.0000i  -0.0298 + 0.0000i  -0.0377 - 0.0000i   0.0813 - 0.0000i
  0.0143 + 0.0000i   0.0674 - 0.0000i  -0.1040 + 0.0000i   0.0781 + 0.0000i
 -0.1543 + 0.0000i  -0.0413 - 0.0000i   0.2057 + 0.0000i  -0.2426 + 0.0000i
  0.2396 - 0.0000i  -0.0552 + 0.0000i  -0.1600 - 0.0000i   0.2718 - 0.0000i
 -0.1636 + 0.0000i   0.1519 - 0.0000i  -0.0402 + 0.0000i  -0.0910 + 0.0000i
 -0.0888 + 0.0000i  -0.1419 + 0.0000i   0.2657 - 0.0000i  -0.2231 + 0.0000i
  0.3860 - 0.0000i  -0.0260 - 0.0000i  -0.3252 - 0.0000i   0.4588 - 0.0000i
 -0.4984 + 0.0000i   0.2705 - 0.0000i   0.1138 + 0.0000i  -0.4017 + 0.0000i
  0.2471 - 0.0000i  -0.3951 + 0.0000i   0.2705 - 0.0000i   0.0064 + 0.0000i
  0.3309 - 0.0000i   0.2143 - 0.0000i  -0.5478 + 0.0000i   0.5175 - 0.0000i
 -0.9208 + 0.0000i   0.2788 - 0.0000i   0.4313 + 0.0000i  -0.7929 + 0.0000i
  1.0440 - 0.0000i  -0.8212 + 0.0000i   0.1388 - 0.0000i   0.5151 - 0.0000i
 -0.3126 + 0.0000i   0.9568 - 0.0000i  -0.8630 + 0.0000i   0.2939 - 0.0000i
 -1.3101 + 0.0000i  -0.2706 - 0.0000i   1.1704 + 0.0000i  -1.1933 + 0.0000i
  3.4045 - 0.0000i  -1.3383 + 0.0000i  -0.5148 - 0.0000i   1.4892 - 0.0000i
 -5.2305 - 0.0000i   3.5096 + 0.0000i  -1.2726 + 0.0000i  -0.6047 + 0.0000i
  6.0558 + 0.0000i  -5.5116 + 0.0000i   3.7858 - 0.0000i  -1.5446 + 0.0000i
 -5.5116 - 0.0000i   6.5497 + 0.0000i  -6.1465 + 0.0000i   4.3936 - 0.0000i
  3.7858 + 0.0000i  -6.1465 - 0.0000i   7.3846 + 0.0000i  -6.9136 + 0.0000i
 -1.5446 - 0.0000i   4.3936 + 0.0000i  -6.9136 - 0.0000i   8.0725 + 0.0000i
```

$\{G_j\}^T = 1.0e+03*\{$0.5886 - 0.0000i -0.9675 + 0.0000i 0.8356 - 0.0000i -0.7224 + 0.0000i 0.7364 - 0.0000i -0.8821 + 0.0000i 1.0805 + 0.0000i -1.2188 - 0.0000i 1.2172 - 0.0000i -1.0769 + 0.0000i 0.8799 - 0.0000i -0.7415 + 0.0000i 0.7425 - 0.0000i -0.8825 + 0.0000i 1.0796 + 0.0000i -1.2187 - 0.0000i 1.2182 - 0.0000i -1.0787 + 0.0000i 0.8817 - 0.0000i -0.7427 + 0.0000i 0.7431 - 0.0000i -0.8825 + 0.0000i 1.0795 + 0.0000i -1.2186 - 0.0000i 0.0000 + 0.0000i$\}$.

$\{A_i\}^T = 1.0e+09*\{$0.0002 - 0.0000i 0.0000 - 0.0000i 0.0001 - 0.0000i 0.0002 - 0.0000i 0.0004 - 0.0001i 0.0012 - 0.0003i 0.0032 - 0.0008i 0.0086 - 0.0022i 0.0217 - 0.0055i 0.0512 - 0.0127i 0.1118 - 0.0271i 0.2231 - 0.0527i 0.4027 - 0.0925i 0.6519 - 0.1455i 0.9379 - 0.2032i 1.1879 - 0.2495i 1.3104 - 0.2667i 1.2436 - 0.2450i 1.0001 - 0.1906i 0.6685 - 0.1231i 0.3617 - 0.0642i 0.1524 - 0.0261i 0.0470 - 0.0077i 0.0095 - 0.0015i 0.0009 - 0.0001i$\}$.